

# The Role of Interfacial Interactions on the Crystallinity and Nanomechanical Properties of Clay–Polymer Nanocomposites: A Molecular Dynamics Study

Debashis Sikdar, Dinesh R. Katti, Kalpana S. Katti

Department of Civil Engineering, North Dakota State University, Fargo, ND 58105

Received 18 May 2007; accepted 30 September 2007

DOI 10.1002/app.27504

Published online 26 November 2007 in Wiley InterScience (www.interscience.wiley.com).

**ABSTRACT:** Polymer clay nanocomposites (PCN) show enhanced mechanical, thermal, liquid or gas barrier properties in comparison to pure polymer. However, the mechanisms for enhancement of these physical properties of PCN are not well understood. This knowledge is important for tailoring the properties of PCN to desired specifications. Our earlier study showed that organic modifiers have significant influence on the crystallinity and nanomechanical properties of PCN. For quantitative evaluation of the influence of organic modifiers on the crystallinity and nanomechanical properties of PCN, molecular models of three intercalated PCNs containing same polymer and clay but with three different organic modifiers are constructed

in this work. Using molecular dynamics simulations, the interaction energies among the different constituents of PCNs are evaluated. This study reveals that the interactions between polymer, organic modifiers, and intercalated clay are critical factors in controlling the crystallinity and enhancement of nanomechanical properties of PCN. We have described the possible mechanisms leading to change in crystallinity and nanomechanical properties. © 2007 Wiley Periodicals, Inc. *J Appl Polym Sci* 107: 3137–3148, 2008

**Key words:** polymer–clay nanocomposites; molecular dynamics simulation; crystallinity; molecular modeling; non-bonded interaction

## INTRODUCTION

In recent years, polymer–clay nanocomposite (PCN) has been a material of interest for researchers because of significantly enhanced mechanical,<sup>1–4</sup> thermal,<sup>5–8</sup> and, liquid and gas barrier<sup>9,10</sup> properties with respect to pristine polymer. Since the development of PCN in 1992 by Toyota research laboratory,<sup>11</sup> different types of PCN have been synthesized employing almost all common types of polymers and using different synthesis techniques. Different PCNs exhibit different amount of improvement in mechanical or thermal properties in comparison to pristine polymer, depending on the constituents of composite, and the type of polymer used in synthesizing the PCN.<sup>12</sup> However, mechanisms leading to the phenomenon of enhancement of physical properties of PCN in comparison to pristine polymer is not well understood, which prevents tailoring the enhancement of properties of particular polymer based PCN to desired levels. This knowledge is important for designing the next-generation novel composite materials with tailored mechanical and thermal properties. In this work, we have described the

mechanisms leading to improvement of mechanical properties of PCN.

The main constituents of PCN are polymer and clay. The expansive clay mineral such as sodium montmorillonite (MMT) is generally used as clay in the synthesis of PCN. MMT is hydrophilic in nature. In synthesizing PCN containing hydrophobic polymer, first MMT is treated with organic modifier for transforming it from hydrophilic to hydrophobic, and organically modified montmorillonite (OMMT) is formed. Mixing OMMT with hydrophobic polymer, the PCN is made. Thus, from the synthesis route of PCN it appears that the primary function of organic modifiers is to enhance the miscibility of MMT with hydrophobic polymer. Ma et al.<sup>13</sup> showed that PCNs synthesized with same polymer and clay but with different organic modifiers result in different mechanical and thermal properties in the bulk scale. In our earlier work,<sup>14</sup> the same phenomenon is observed. PCNs synthesized with same polymer, Polyamide 6 (PA6) and MMT but with three different organic modifiers (12-aminolauric acid, *n*-dodecylamine, and 1,12-diaminododecane) result in different amounts of enhancement in nanomechanical properties (elastic modulus, loss modulus, storage modulus, and loss factor in the nanometer length scale) and crystallinity. Thus, it appears that organic modifiers have significant influence on the microstructure as well as enhancement of physical properties of PCN.

Correspondence to: D. R. Katti (dinesh.katti@ndsu.edu).

The properties of composites are largely influenced by the interactions between constituents.<sup>15</sup> Molecular dynamics (MD) is a useful technique for studying the structure, dynamics, and interphasial interactions between different constituents of PCN.<sup>16</sup> Zeng et al. studied the conformation of organic modifiers in intercalated OMMT using MD simulations technique.<sup>17</sup> Tanaka et al. evaluated the binding energy between clay and polymer in the exfoliated PCN using MD.<sup>18</sup> Gaudel-Siri<sup>19</sup> investigated the intercalation process in PCN using MD simulation. In a separate study, Vaia and Giannelis<sup>20</sup> studied the interactions between the constituents of PCN with varying molecular weight of polymer and processing temperature. Balazs and coworkers<sup>21,22</sup> studied the intercalation mechanism of PCN using density functional theory. In our earlier work,<sup>23</sup> a representative intercalated model of PCN containing PA6 as polymer, 12-aminolauric acid as organic modifier, and MMT as clay was constructed. In a separate work,<sup>24</sup> using that representative model of intercalated PCN, interaction between the different constituents of a PCN was evaluated.

Thus, significant work has been done to evaluate the structure and properties of PCN; however, little progress has been achieved toward uncovering the mechanisms behind the property enhancement of PCN. Hence in this work, we have constructed molecular models of three intercalated PCNs, which were studied for crystallinity and nanomechanical properties in our previous work.<sup>14</sup> We know that interaction energies are a measure of interaction between the different constituents of PCN. Hence using MD simulation, the interaction energies between the constituents in different PCNs have been evaluated, which provides estimation of the interaction between different phases in PCNs. In this work, comparing the interphasial interactions with the crystallinity and nanomechanical properties of PCNs, important insight is obtained regarding the microstructure, and mechanisms responsible for the enhancement of nanomechanical properties of PCN. Our study reveals that organic modifiers play an important role in controlling the microstructure and physical properties of PCN.

## COMPUTATIONAL METHODOLOGY

Molecular dynamics simulation has been used in this work for studying the interactions between the different constituents of OMMT and PCN. In this study, three different organic modifiers, 12-aminolauric acid, *n*-dodecylamine, and 1,12-diaminododecane have been used for making three different OMMTs. The polymer used for synthesizing the PCN is PA6. The structure of polymer, clay, and or-

ganic modifiers are constructed using the module Builder<sup>TM</sup> of InsightII 2005 of Biosym Technologies, San Diego, CA. The force field parameters used for polymer and organic modifiers are CHARMM 27.<sup>25</sup> For the atoms in polymer and organic modifiers, the standard partial charges obtained from library of CHARMM 27 have been used. In the synthesis of OMMT, all organic modifiers are protonated by treating them with hydrochloric acid in the aqueous solution. The protonation of organic modifiers turns the end functional amine group (NH<sub>2</sub>) into protonated amine group (N<sup>+</sup>H<sub>3</sub>), and imparts a net positive charge of +1 in each protonated amine group present in the molecule of each organic modifier used in this work. Accordingly, the net charge per molecule of 12-aminolauric acid and *n*-dodecylamine is +1. The net charge in each molecule of 1,12-diaminododecane after protonation is +2 because of two protonated amine groups in each molecule of 1,12-diaminododecane. The partial charges on the atoms of polymer and organic modifiers are shown in Figure 1. The unit cell of isomorphically ion-substituted MMT used in this work is [NaSi<sub>16</sub>(Al<sub>6</sub>FeMg)O<sub>40</sub>(OH)<sub>8</sub>]. MMT has the standard T-O-T structure in which aluminum octahedral layer is sandwiched between two silica tetrahedral layers. The coordinates of atoms of MMT unit cell are obtained from the model of Skipper et al.<sup>26,27</sup> The charges on the atoms of MMT are obtained from the work of Teppen et al.<sup>28</sup> In our earlier work,<sup>29</sup> the CHARMM force field parameters for MMT were derived, and those parameters have been used in the present work for clay. The molecular structures of polymer and organic modifiers are minimized initially using InsightII, and those energy-minimized structures are used for making the initial models of OMMT and PCN using VMD.<sup>30</sup> The OMMTs synthesized using organic modifiers, 12-aminolauric acid, *n*-dodecylamine, and 1,12-diaminododecane are referred to in this article as OMMT-lauric, OMMT-dodecyl, OMMT-dodecane, respectively. Likewise the PA6-based PCN synthesized using OMMT-lauric, OMMT-dodecyl, OMMT-dodecane are referred to in this work as PCN-lauric, PCN-dodecyl, PCN-dodecane, respectively. The synthesis procedure of different OMMTs and PCNs is described in our earlier work.<sup>14,31</sup>

## SIMULATION DETAILS OF OMMT AND PCN MODEL

Molecular dynamics software, NAMD 2.5,<sup>32</sup> has been used for conducting MD of OMMT and PCN. The Varlet algorithm is used for conducting MD. The isothermal-isobaric ensemble, constant number, pressure, and temperature (NPT) simulation is applied to the MD simulation. For accounting the

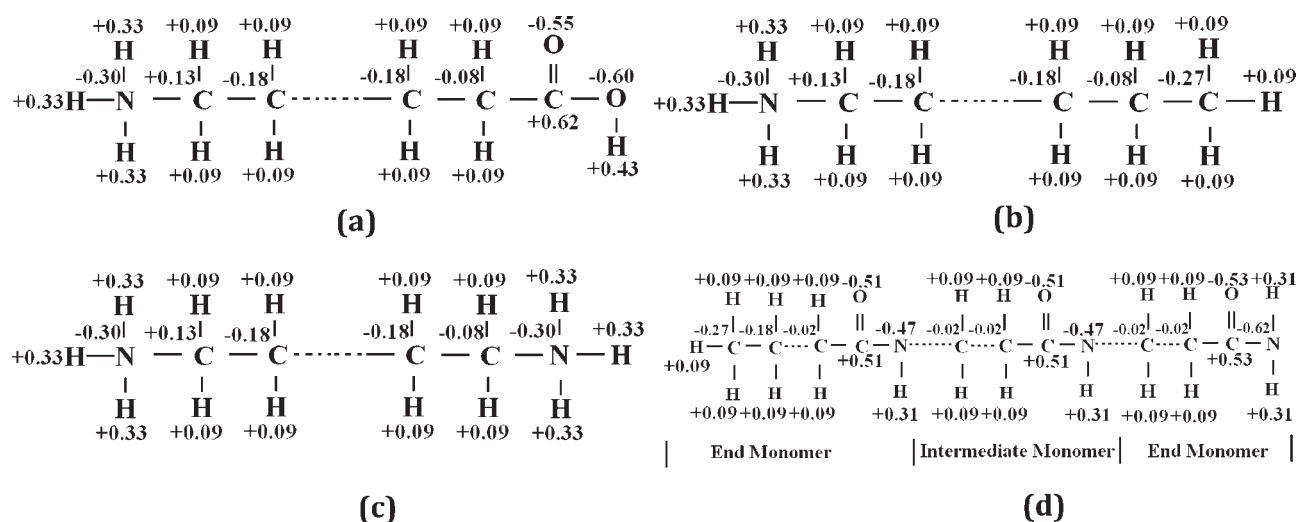


**Figure 1** Molecular structure and partial charges on the atoms of (a) 12-aminolauric acid, (b) *n*-dodecylamine, (c) 1,12-diaminododecane, (d) polyamide 6.

van der Waals interaction, switch and cut off distances are incorporated, which are 14 and 16 Å, respectively, in all OMMT and PCN models. For incorporating electrostatic interaction, Particle Mesh Ewald simulation method is used.<sup>33</sup> The Nosé-Hoover Langevin piston method is used for controlling pressure; and, Langevin dynamics is used for controlling the temperature in the simulation.<sup>34,35</sup> The variation of temperature in the MD simulation is maintained, matching the synthesis route of OMMT. First, the OMMT model is minimized for a duration of 5 pico seconds (ps) ( $10^{-12}$  s) at 0 K temperature under vacuum. The time step used in the simulation is 0.5 fs. Then, MD of OMMT is conducted by increasing the temperature of the system to 300 K under vacuum. Keeping the temperature at 300 K, the pressure of the system is increased to 1 atmospheric (1.013 bar) pressure in four equal steps to bring the temperature and pressure of the OMMT model to ambient condition. Then, keeping the pressure at 1 atmospheric level, the temperature of the OMMT model is further raised to 333 K, and subsequently it is brought down to the temperature of 300 K. In each step of change of temperature and pressure, the simulation is run for 25 ps. Finally, the OMMT model is run for a duration of 200 ps at room temperature and pressure for attaining the equilibrium of the OMMT model. The energy versus time plot of the OMMT model shows that the simulation time of 200 ps is sufficient to equilibrate the model. A force constraint of  $1 \text{ kcal mol}^{-1} \text{ \AA}^{-1}$  is applied to all the atoms of MMT in the *x* and *y* directions, keeping *z*-direction movement of MMT free. No constraining force is applied on the atoms of organic modifiers.

The simulation procedure of PCN model is similar to OMMT, except the maximum temperature used in the simulation of PCN. The maximum temperature

used here is 300 K matching the synthesis route of PCN samples.<sup>14,31</sup> Similar to the simulation of OMMT models, in every step of change of pressure and temperature during MD of PCN models, simulation is conducted for duration of 25 ps. Finally, the whole PCN model is run for 200 ps to equilibrate the model. As before, the energy versus time plot shows that the 200-ps duration of simulation is sufficient for convergence of energy in the PCN model. A force constraint of  $1 \text{ kcal mol}^{-1} \text{ \AA}^{-1}$  is applied to all the atoms of MMT in the *x* and *y* direction, keeping the atoms of polymer and organic modifiers unconstrained in all the directions. Additional details about computational methodology and simulation procedure can be found in our earlier work.<sup>23,24</sup>

## MODEL CONSTRUCTION

### Model of organically modified montmorillonite

The construction of models of OMMT has been done by comparing the experimental results of X-ray diffraction (XRD) and photoacoustic Fourier transform infrared spectroscopy (PA-FTIR) with modeling criteria as presented in detail in our earlier work.<sup>23</sup> There are 18 periodically replicated unit cells of MMT in each layer of the intercalated model of OMMT, which have a net charge of  $-9$ . Adequate number of organic modifiers are incorporated in the interlayer clay gallery of MMT to make the whole OMMT model charge neutral. The PA-FTIR study of OMMT shows that there are no water molecules in the interlayer of OMMT,<sup>31,36</sup> and hence, in our initial model of OMMT, no water molecules are incorporated. The initial alignment of organic modifiers is parallel to the interlayer surface of MMT. From the

**TABLE I**  
***d*-Spacing of OMMT Obtained from XRD and MD Simulation**

Sample	<i>d</i> -spacing from XRD (Å)	<i>d</i> -spacing from MD simulation (Å)
OMMT-lauric	15.60	15.85
OMMT-dodecyl	14.18	14.72
OMMT-dodecane	13.36	13.85
MMT	11.11	–

FTIR study of OMMTs,<sup>31,36</sup> it is further observed that there are no bonded interactions between MMT and organic modifiers in all three OMMTs. Hence, in the model of OMMTs, no bond is incorporated between the MMT and organic modifiers. Periodic boundary conditions are applied in the OMMT models in the *x*, *y*, and *z*-directions to replicate the periodic structure of clay in all directions. The initial *d*-spacing of OMMT models are selected as described in our earlier work.<sup>23</sup> Following the synthesis route of OMMT,<sup>14,31</sup> the MD simulation of initial model of OMMT is conducted for obtaining the final model of OMMT. For selecting the representative model of OMMT, following conditions are applied similar to our earlier work<sup>23</sup>:

1. The final *d*-spacing of molecular model of OMMT matches the experimental *d*-spacing of respective OMMT obtained from XRD result.
2. The OMMT model satisfies the minimum energy conformation.

Running the MD simulation of the initial models of OMMT and incorporating the above two conditions, the final model of OMMTs are obtained. The *d*-spacings of the final model of OMMTs obtained

from XRD and MD simulation are shown in Table I. The representative models of OMMTs are shown in Figure 2.

### Model of polymer–clay nanocomposite

The construction of PCN models is done using the procedure described in our early work where the results from experiments (XRD and PA-FTIR) and MD simulation were combined.<sup>23</sup> The initial intercalated models of PCNs containing three different OMMTs are obtained by inserting the energy-minimized structure of polymer (PA6) into interlayer clay gallery of the respective OMMT models. To get the globally minimized structure of polymer, polymer of different chain length are annealed at higher temperature as presented in detail in our earlier work.<sup>23</sup> These annealed polymers are used for building the initial model of PCNs. The PA-FTIR study of PCN does not show any bonded interactions between polymer, clay, and organic modifiers lying in PCN. Hence, for the construction of PCN models, no bonded interactions have been incorporated between different constituents of PCN. In obtaining the final representative models of PCNs, the following criteria are imposed similar to our previous work<sup>23</sup>:

1. In the initial model of PCN, size and shape of the energy-minimized conformation of annealed polymer fit perfectly in the interlayer clay spacing of final OMMT model.
2. The final *d*-spacing of PCN matches the *d*-spacing observed from XRD of PCN samples.
3. The representative model of PCN sample satisfies the minimum energy conformation.

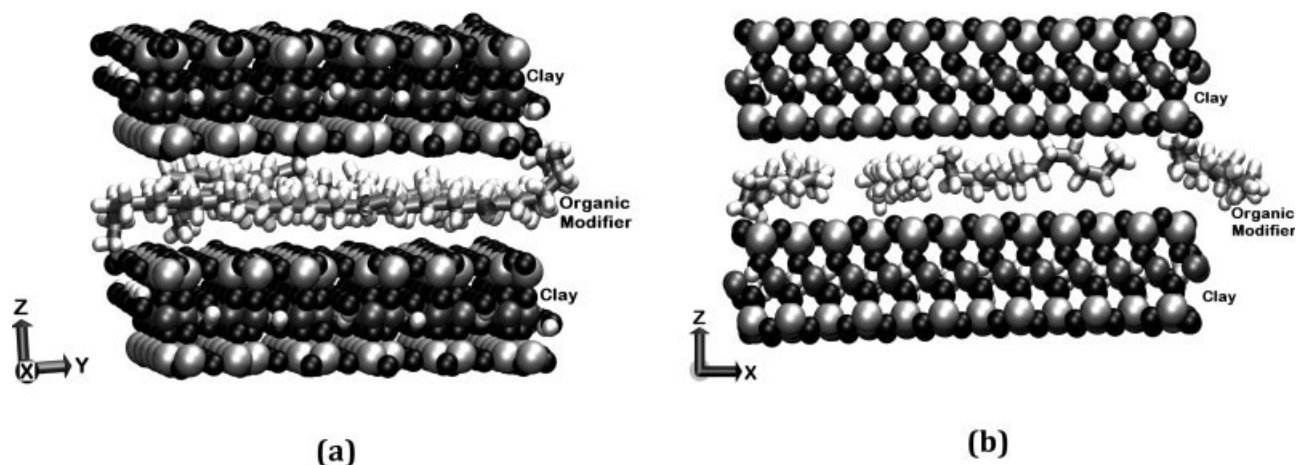


**Figure 2** (a) Molecular model of intercalated organically modified montmorillonite containing sodium montmorillonite and organic modifier, *n*-dodecylamine in the interlayer clay gallery, (b) Representative molecular model of intercalated organically modified montmorillonite containing sodium montmorillonite and organic modifier, 1,12-diaminododecane in the interlayer clay spacing. Clay is in VDW rendering form, and organic modifier is in licorice rendering form.

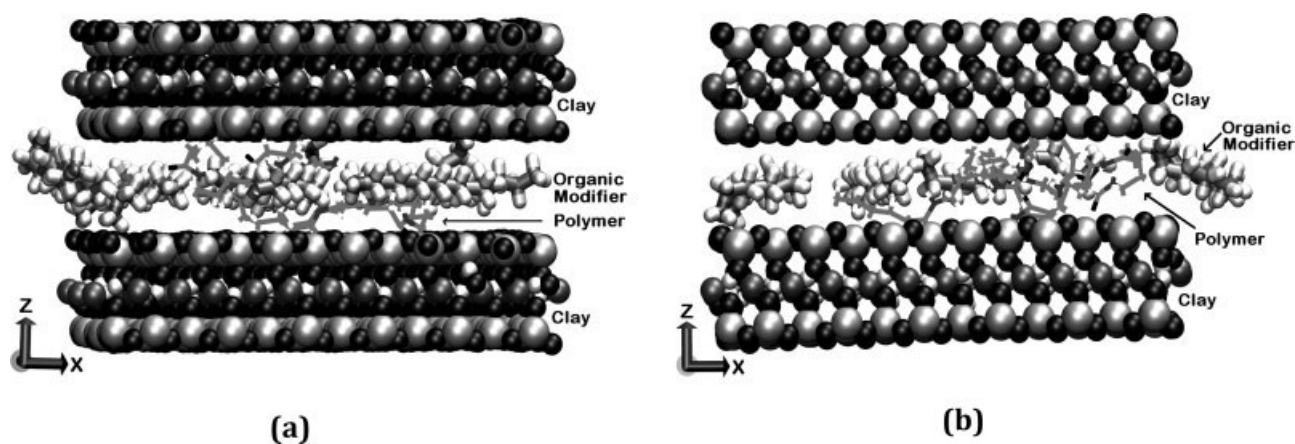


**Figure 3** (a) Molecular model of intercalated polymer-clay nanocomposite containing polyamide 6, sodium montmorillonite and organic modifier, *n*-dodecylamine in the interlayer clay gallery, (b) Molecular model of intercalated polymer-clay nanocomposite containing polyamide 6, sodium montmorillonite, and organic modifier, 1,12-diaminododecane in the interlayer clay spacing. Clay is in VDW rendering form, organic modifier is in licorice rendering form, and polymer is in line rendering form.

The PCN model containing largest polymer chain in the interlayer clay gallery and satisfying the above three conditions is considered the representative intercalated model of PCN. The spatial dimensions of the PCN models are  $33.55 \text{ \AA} \times 28.902 \text{ \AA}$ , whereas in reality micron-size clay sheets exist in PCNs. To overcome the size effect of clay sheet in PCN model, the simulation cell for the PCN models are replicated in all three directions through cellBasisVectors, which are maintained at 40 and 34 in the *x*, and *y* directions, respectively. The cellBasisVector of the PCN models in the *z*-direction is set twice the *d*-spacing of the respective initial PCN model. For Van der Waals interaction, the switch and cut off distances for this model used are 14 and 16  $\text{\AA}$ , respectively. Conducting MD simulation following the synthesis procedure of PCN, and satisfying the above-mentioned conditions, the representative model of PCNs are obtained, which are shown in Figure 3. In all three cases of PCNs, the representative PCN models contain eight-monomer chain intercalated polymer. The *d*-spacing of the PCNs obtained from modeling and XRD is given in Table II, which shows good agreement between the modeling and experimental results. From literature,<sup>37,38</sup> we have seen that the PCN can have *d*-spacing smaller than that of OMMT. From nanoindentation and nanodynamic mechanical experiments,<sup>14</sup> the nanomechanical

properties (elastic modulus, storage modulus, loss modulus, loss factor) of PCNs are found significantly higher than pristine polymer, which indicates the formation of polymer-clay nanocomposite. The final models of PCNs are used for studying the interactions between different constituents of PCNs.

#### CALCULATION OF INTERACTION ENERGY

Using the energy evaluation tool, MDenergy™ of NAMD, the interaction energies between different constituents of composites are found. From structural information, interaction parameters, cutoff and switch distance, the interaction energies of any given set of atoms or between two given sets of atoms for a particular time span can be calculated using the trajectory file of molecular system. The trajectory file of the whole molecular model is directly obtained from MD simulation. The interactions energies for any molecular system can be calculated for bonded and nonbonded energies separately. Further, the bonded energies can be computed in the category of bond, angle, and dihedral energies in the molecular system. Similarly, the nonbonded energy can be computed by splitting into van der Waals, and electrostatic energies for any given set of atoms or between two sets of interacting atoms. All MD simulations of OMMT and PCN are run for duration of 200 ps in the final stage to equilibrate the models. The average of results for last 25 ps was considered for calculating the bonded and different nonbonded energies of the molecular models.

#### RESULTS AND DISCUSSION

Interaction energies are the measure of interactions between different constituents of composites. The

**TABLE II**  
*d*-Spacing of PCN Obtained from XRD and MD Simulation

Sample	<i>d</i> -spacing from XRD ( $\text{\AA}$ )	<i>d</i> -spacing from MD simulation ( $\text{\AA}$ )
PCN-lauric-9%	13.49	14.04
PCN-dodecyl-9%	14.52	14.83
PCN-dodecane-9%	13.71	14.04

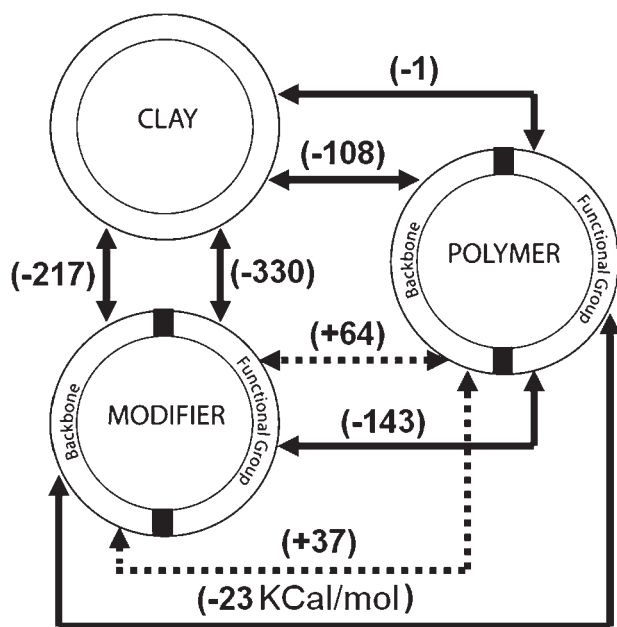


**Figure 4** Interaction energies in kcal/mol between different parts of polymer, organic modifier, and clay in PCN-lauric. Positive energy represents repulsive interaction and negative energy represents attractive interaction.

negative energy indicates attractive interaction, and positive energy represents repulsive interaction between two constituents of composites.

The change in the crystallinity and nanomechanical properties of PA6-based PCNs have been reported in our earlier work.<sup>14</sup> In that work, it is observed that nanomechanical properties (elastic modulus, loss modulus, storage modulus, loss factor) in PCNs increase progressively in the order of PCN-lauric, PCN-dodecyl, and PCN-dodecane; whereas the crystallinity in the PCNs increases exactly in the reverse order. Hence, it appears that with the decrease in crystallinity of PCN, the nanomechanical properties in PCN increase. In this work, different PCNs are synthesized with identical polymers (PA6) and clay (MMT) but with three different organic modifiers. Hence, it appears that organic modifiers have specific influence on the crystallinity and nanomechanical properties of PCN.

### Interactions in PCN-lauric

Using PA-FTIR, the PCN and the individual constituents were studied in our earlier work.<sup>31,36</sup> The work revealed that there are only nonbonded interactions between clay, polymer, and organic modifiers in PCN. Hence in this study, we have evaluated the nonbonded interactions between the different constituents in PCN. The polymer and organic modifier have two parts in their structure (1) functional group, and (2) backbone chain. In the assessment of

interactions between constituents of PCN, the interactions coming from different parts of polymer and organic modifiers have been computed in this work. Figure 4 shows the schematic representation of the nonbonded interactions between different constituents of PCN-lauric. The magnitude of interactions in kcal/mol is indicated in parenthesis adjacent to the respective arrows in the energy diagram. The attractive interactions are represented with solid line, and repulsive interactions are represented in dotted lines in the energy map. From the Figure 4, it is observed that backbone and functional group of organic modifiers both have significant attractive interactions ( $-217$  and  $-330$  kcal/mol, respectively) with clay in PCN-lauric. Whereas between polymer and clay, the main attractive interactions come from the backbone of polymer only which is  $-108$  kcal/mol, the functional group of polymer has very weak interaction ( $-1$  kcal/mol) with clay. The back bone and functional group of polymer and organic modifier both have attractive interactions with clay. However in case of interaction between different parts of polymer and organic modifier, the functional groups of polymer have only attractive interactions with different parts of the modifier. The backbone of polymer has repulsive interactions with backbone and functional group of organic modifier. In terms of magnitude, the strongest attractive interactions are found between the clay and modifiers, followed by interactions between clay and polymer. The attractive interactions between polymer and modifier are lowest among all interactions in PCN. The highest interactions are between functional groups of organic modifiers and clay, and between backbone of modifier and clay. This interaction is dominantly electrostatic in nature. The partial charges on the atoms of functional groups of organic modifier are relative higher and those result in dominantly electrostatic interactions in PCN. Although the partial charges on the backbone atoms are relatively lower, however, the larger number of atoms present in the backbone of organic modifier contributes to very significant interactions as evident from Figure 4.

### Interactions in PCN-dodecyl

The interaction energies between different constituents of PCN-dodecyl are shown in the Figure 5. The interaction energies show the identical trend as seen in PCN-lauric. All the interactions are attractive in nature except the interactions of backbone of polymer with backbone and functional group of modifier. In PCN-lauric, between the functional group of polymer and clay there are almost no interactions ( $-1$  kcal/mol); however, the interaction in PCN-dodecyl is much higher, which is  $-26$  kcal/mol. In PCN-dodecyl, the highest component of interaction

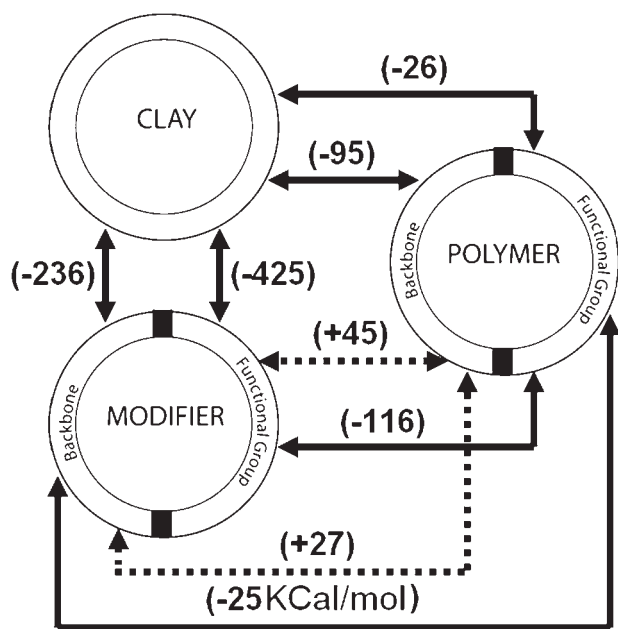


**Figure 5** Interaction energies in kcal/mol between different parts of polymer, organic modifier, and clay in PCN-dodecyl. Positive energy represents repulsive interaction and negative energy represents attractive interaction.

is observed between the functional groups of modifier and clay. The functional group of polymer has almost equal attractive interactions with clay and backbone of modifier; and these two are the lowest attractive interactions in PCN-dodecyl.

### Interactions in PCN-dodecane

The mapping of interaction energies between different components of PCN-dodecane is shown in Figure 6. Energy diagram has the same trend of interactions as are seen in PCN-lauric and PCN-dodecyl. The interactions between clay and modifier are highest, followed by clay-polymer and polymer-modifier. All interactions are attractive in nature except the interactions of backbone of polymer with backbone and functional groups of organic modifier, which is repulsive in nature. Both positive and negative interactions have significant role on the crystallinity of PCN and consequently mechanical properties of PCNs.

### Comparison of interactions between polymer and modifier in PCNs

In PCNs, polymer is the most abundant constituent in terms of volume and mass. Hence in determining the crystallinity and properties of PCN, the interactions of polymer with other constituents of PCN would have significant impact. The PCNs in this work are composed of identical polymer and clay but with different organic modifiers. Thus, interac-

tions between polymer and organic modifier could be very important in the resulting differences in crystallinity and mechanical properties observed in the PCNs. The molecule of protonated 12-aminolauric acid has 11 methylene units ( $(\text{CH}_2)_{11}$ ) in the backbone chain; and one protonated amine group ( $\text{NH}_3$ ) and one carboxylic group ( $\text{COOH}$ ) as the two end functional groups. In the molecule of protonated *n*-dodecylamine, there are 11 methylene units in the backbone chain; and one protonated amine group and one methyl group ( $\text{CH}_3$ ) as the two end functional groups. In the molecular structure of protonated 1,12-diaminododecane, there are 12 methylene units in the backbone chain and two protonated amine groups as the two end functional groups. Thus, comparing the molecular structure of three organic modifiers, it is seen that the structure of organic modifiers is almost same except for functional group of modifiers at one end. Hence, the interactions between functional groups of modifier and polymer may have significant role in the differences in crystallinity and nanomechanical properties in the three PCNs.

The comparison of interactions between different parts of polymer and organic modifiers in the three PCNs is shown in Table III. From column 1 of Table III, it is evident that functional group of modifier has significantly strong attractive interactions with the functional group of polymer. It appears that the functional groups of polymer and organic modifiers act as nonbonded docking sites to each other, result-

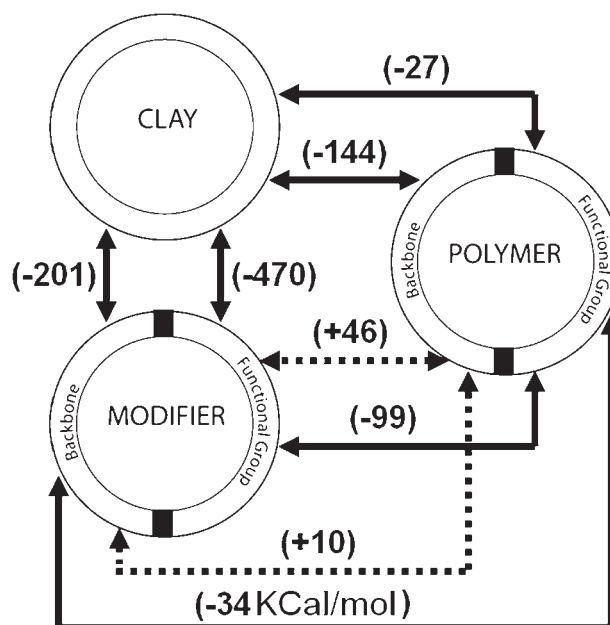


**Figure 6** Interaction energies in kcal/mol between different parts of polymer, organic modifier, and clay in PCN-dodecane. Positive energy represents repulsive interaction and negative energy represents attractive interaction.

TABLE III  
Components of Interactions Between Modifier and Polymer in PCNs Containing Different Organic Modifiers

Sample	Modifier backbone-polymer functional group (kcal/mol)	Modifier polymer functional group (kcal/mol)	Modifier functional group-polymer backbone (kcal/mol)	Modifier backbone-polymer backbone (kcal/mol)	Modifier polymer functional group (kcal/mol)	Modifier functional group-polymer backbone (kcal/mol)	Modifier-polymer backbone (kcal/mole)
PCN-lauric-9%	-23	-143	-166	+37	-166	+64	+101
PCN-dodecyl-9%	-25	-116	-141	+27	-141	+45	+72
PCN-dodecane-9%	-34	-99	-133	+10	-133	+46	+56

ing in strong attractive interactions between functional group of polymer and whole organic modifiers as seen in column 2 of Table III. The “docking strength” (defined as magnitude of attractive interaction energy) varies from strongest to weakest in the order of PCN-lauric, PCN-dodecyl, and PCN-dodecane as seen from Table III. On the other hand, as seen in columns 3 and 4 of Table III, it is observed that polymer backbone has significantly strong repulsive interactions with functional groups and backbone of modifiers. The magnitude of total repulsive interaction of backbone of polymer with modifier in PCNs follows the same order as above as seen from the Table III. Because of strong attractive interactions of the functional groups and simultaneous repulsive interactions of backbone of polymer with modifiers, the normal conformation of polymer is disrupted in the interlayer clay gallery of PCN. We define this disturbance in confirmation of the polymer as a result of attractive interactions at functional groups and simultaneous repulsion of the backbone chain of the polymer as “ripple action.” A schematic representation of intercalated polymer subjected to localized attractive and repulsive forces is illustrated in Figure 7. Stronger the differences in attractive and repulsive interaction, greater will be the “ripple action” in polymer, greater will be the disruption of crystallinity of polymer in the PCNs. PCN-lauric has the strongest docking (attractive) interaction between functional group of polymer and modifier as well as highest repulsive interactions between backbone of polymer and modifier, producing the greatest disruption in structure of polymer and consequently resulting in the lowest crystallinity among the three PCNs as observed in our earlier work.<sup>14</sup> The PCN-dodecyl has the next stronger “ripple action” resulting in the next higher crystallinity. In PCN-dodecane, attractive interactions of polymer functional group and repulsive interactions of polymer backbone chain with modifier are smallest in magnitude among the three PCNs. This least intense “ripple action” results in the least disruption of crystallinity in polymer and subsequently imparts the highest crystallinity in PCN-dodecane among all three PCNs.

The intercalated PCN is shown schematically in Figure 8(a), where it is observed that intercalated clay particles are dispersed in the polymer matrix uniformly. The ovals surrounding the intercalated clay schematically represent the zone of influence of clay within which the crystallinity of polymer is significantly disrupted by the nanoclay fillers and organic modifiers. The polymer outside the oval zone represents the portion of polymer unperturbed by the interaction of intercalated clay particles.

A zoomed in schematic view of a typical intercalated clay particle is shown in Figure 8(b) where we



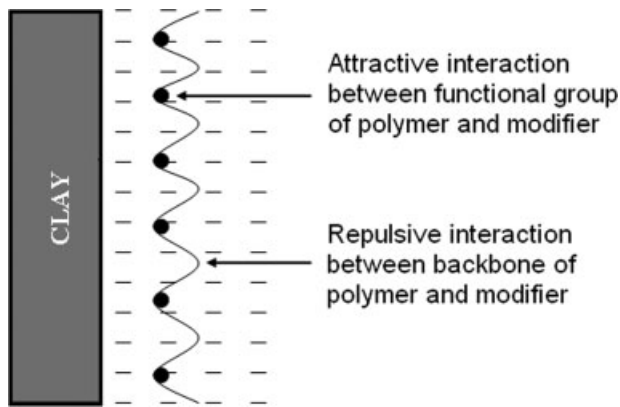


**Figure 7** Ripple action in the intercalated polymer due to interaction with organic modifier.

see that because of “ripple action,” the crystallinity of polymers inside the clay gallery and some part of polymers outside the clay gallery could be disrupted. The nanoclay fillers are uniformly dispersed in the polymer matrix of PCN. It appears that the well dispersed intercalated nanoclay particles by its physical presence also disrupt the crystallinity of polymer matrix in the PCN.

Higher the nanoclay loading, larger will be the number of intercalated clay blocks in the PCN. With the increase of intercalated clay blocks, crystallinity of more amount of polymer intercalated as well as adjacent to clay will be disrupted. Thus it appears that with the increase of clay loading, because of interactions between polymer and modifier and influence of charge surface of clay, the crystallinity of PCNs would decrease. From our earlier work,<sup>14</sup> to

investigate the effect of nanoclay loading on the crystal structure and nanomechanical properties of PCN, the PCN samples were synthesized containing identical polymer (PA6) and organic modifier (12-aminolauric acid) but with three different nanoclay loading (3, 6, and 9% of weight of polymer). From that study it is seen that in PCN-lauric with increasing nanoclay loading from 3 to 9 wt %, the crystallinity in PCN reduces significantly, which is consistent with mechanisms described earlier.

The interaction energy between different constituents of PCN has significant impact on the mechanical properties of composites. The negative interaction energy indicates the stable attractive interactions between the interacting constituents of composites. The three PCNs differ from each other due to the presence of different organic modifiers, more precisely the different end functional groups as mentioned in the Section “Comparison of interactions between polymer and modifier in PCNs.” Therefore it appears that the interactions of functional groups of modifier with polymer are important in determining the mechanical properties of PCNs. The most significant interactions are found between the functional groups of polymer with functional groups of organic modifiers. These interactions in all of the PCNs are attractive in nature and impart the docking action of intercalated polymer on the organic modifiers inside the clay gallery. Hence it is expected that polymer with stronger docking will result in higher mechanical properties. As seen from Table III, PCN-lauric has the strongest docking actions between the functional group of polymer and functional group of modifier as well as whole

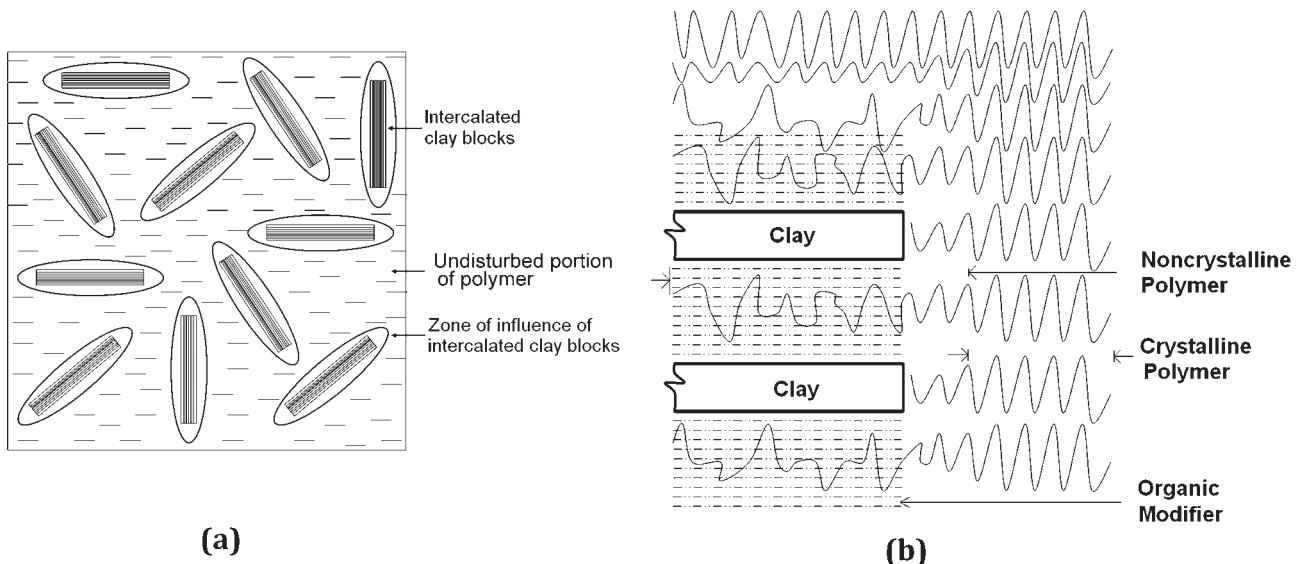


**Figure 8** (a) Schematic representation of intercalated PCN showing the influence of clay surface on the crystallinity of polymer outside the clay gallery, (b) the schematic representation shows the disruption of polymer in and outside the clay gallery in PCN.

TABLE IV  
Interactions of Clay and Polymer in PCNs Containing Different Organic Modifiers

Sample	Clay-polymer backbone			Clay-polymer functional group			Clay-polymer		
	VDW <sup>a</sup> (kcal/mol)	Electrostatic (kcal/mol)	Total nonbond (kcal/mol)	VDW (kcal/mol)	Electrostatic (kcal/mol)	Total nonbond (kcal/mol)	VDW (kcal/mol)	Electrostatic (kcal/mol)	Total nonbond (kcal/mol)
PCN-lauric-9%	-76	-32	-108	-33	+32	-1	-109	0	-109
PCN-dodecyl-9%	-71	-24	-95	-34	+8	-26	-105	-16	-121
PCN-dodecane-9%	-111	-33	-144	-74	+47	-27	-185	+14	-171

<sup>a</sup> VDW = van der Waals.

organic modifier, and hence results in the highest nanomechanical properties between the three PCNs. The next stronger interactions are observed in PCN-dodecyl followed by PCN-dodecane resulting in next higher nanomechanical properties.

#### Comparison of interactions between clay and polymer in PCNs

The interactions between different parts of polymer and clay in different PCNs are shown in Table IV. The functional groups of polymer have relatively weaker interactions with clay. There are comparatively stronger interactions between backbone of polymer and clay as seen from Table IV. Further, it is observed that the electrostatic portion of interactions between backbone of polymer and clay does not differ significantly. The difference of interactions between backbone of polymer and clay is primarily due to the van der Waals interactions, which depend on the distance between the interacting atoms. The backbone of polymer has significant repulsive interaction with organic modifier. Different modifiers result in different amount of repulsive interactions with backbone chain of polymer, which consequently result in dissimilar distances between polymer and clay in different PCNs resulting in the different van der Waals energy between clay and polymer. In all the PCNs, same clay and polymer with identical size have been used. Hence the localized interaction between polymer and clay are a result of influence of the organic modifier. For a given amount of clay loading, the differences in mechanical properties observed for the different modifiers are the result of polymer modifier interactions.

#### Comparison of interactions between clay and modifier in PCNs

The interactions between clay and organic modifiers are shown in Table V. From Table V, it is evident that the functional group and backbone chain of organic modifiers both have attractive interactions with clay. Because of high partial charges on the atoms of functional groups on modifiers, it has dominantly electrostatic interaction with clay. The backbones of organic modifiers have dominantly van der Waals interaction with clay. Generally interface is the weakest point of composite materials. Comparing the results of Tables III and V, it is observed that interactions between clay and organic modifier are much stronger than the interactions between polymer and modifier. Since modifier-clay interactions are significantly higher than polymer-modifier interaction, the polymer-modifier interactions play a controlling role in the mechanical properties of PCNs.

**TABLE V**  
**Components of Interactions Between Modifier and Clay in PCNs Containing Different Organic Modifiers**

Sample	Clay-modifier backbone			Clay-modifier functional group			Clay-modifier		
	VDW <sup>a</sup> (kcal/mol)	Electrostatic (kcal/mol)	Total nonbond (kcal/mol)	VDW (kcal/mol)	Electrostatic (kcal/mol)	Total nonbond (kcal/mol)	VDW (kcal/mol)	Electrostatic (kcal/mol)	Total nonbond (kcal/mol)
PCN-lauric-9%	-113	-104	-217	-45	-285	-330	-158	-389	-547
PCN-dodecyl-9%	-135	-101	-236	-28	-397	-425	-163	-498	-661
PCN-dodecane-9% (4.5 no. of modifiers)	-95	-106	-201	+7	-477	-470	-88	-583	-671

<sup>a</sup> VDW = van der Waals.

**TABLE VI**  
**Comparison Between Crystallinity and Mechanical Properties with Components of Interactions Between Modifier and Polymer in PCNs Containing Different Organic Modifiers**

Sample	Modifier-polymer functional group (kcal/mol)	Modifier-polymer backbone (kcal/mol)	% Crystallinity <sup>14</sup>	Elastic modulus E (GPa) <sup>14</sup>	Storage modulus E' (GPa) <sup>14</sup>	Loss modulus E'' (GPa) <sup>14</sup>	Loss factor (tan δ) <sup>14</sup>
PCN-lauric-9%	-166	+101	23.05	5.460	5.445	0.634	0.12
PCN-dodecyl-9%	-141	+72	24.71	4.766	4.801	0.446	0.09
PCN-dodecane-9%	-133	+56	25.52	4.417	4.544	0.374	0.08
Pure PA6			27.61	3.352	3.482	0.258	0.07

Comparing interactions between different parts of polymer and organic modifier with the crystallinity and nanomechanical properties of PCNs as shown in Table VI, it appears that attractive interactions between functional group of polymer with organic modifier as well as repulsive interactions between backbones of polymer with organic modifier control the crystallinity and nanomechanical properties of PCNs.

## CONCLUSIONS

Organic modifiers influence the crystallinity and nanomechanical properties of PCN due to differences in interactions between constituents. The interactions between the polymer and organic modifier are the controlling factors influencing the crystallinity and nanomechanical properties of PCN. Attractive interactions between the functional groups of polymer and modifier and simultaneous repulsive interactions between modifier and backbone of polymer result in conformational changes in polymer, which causes disruption of periodicity of polymer manifesting in changes in crystallinity of polymer in PCN. Higher the level of these disruptive interactions, lower the crystallinity of polymer in the PCN and higher the nanomechanical properties. The pinning action of polymer functional groups with modifiers as a result of attractive interactions are related to the nanomechanical properties of PCN, with nanomechanical properties increasing with increased attractive interactions.

The authors would like to acknowledge the use of computational resources at the Center for High Performance Computing (CHPC), NDSU and Biomedical Research Infrastructure Network (BRIN). The authors thank Dr. Gregory H. Wettstein for his assistance in providing hardware and software facilities. Author DS acknowledges the support of NDSU doctoral fellowship award.

## References

1. Chaudhary, D. S.; Prasad, R.; Gupta, R. K.; Bhattacharya, S. N. *Thermochim Acta* 2005, 433, 187.
2. Yuana, Q.; Misra, R. D. K. *Polymer* 2006, 47, 4421.
3. Tannirua, M.; Yuana, Q.; Misra, R. D. K. *Polymer* 2006, 47, 2133.
4. Zhang, M.; Sundararaj, U. *Macromol Mater Eng* 2006, 291, 697.
5. Yeh, J. M.; Chen, C. L.; Huang, C. C.; Chang, F. C.; Chen, S. C.; Su, P. L.; Kuo, C. C.; Hsu, J. T.; Chen, B.; Yu, Y. H. *J Appl Polym Sci* 2006, 99, 1576.
6. Wua, D.; Zhoua, C.; Fana, X.; Maob, D.; Bian, Z. *Polym Degrad Stab* 2005, 87, 511.
7. Zhang, J.; Jiang, D. D.; Wang, D.; Wilkie, C. A. *Polym Adv Technol* 2005, 16, 800.
8. Diagnea, M.; Guèyea, M.; Vidalb, L.; Tidjani, A. *Polym Degrad Stab* 2005, 89, 418.
9. Choi, W. J.; Kim, H. J.; Yoon, K. H.; Kwon, O. H.; Hwang, C. K. *J Appl Polym Sci* 2006, 100, 4875.
10. Pramanik, M.; Srivastava, S. K.; Biswas, K. S.; Bhowmick, A. K. *J Appl Polym Sci* 2003, 87, 2216.
11. Okada, A.; Kawasumi, M.; Usuki, A.; Kojima, Y.; Kurauchi, T.; Kamigaito, O. *Mater Res Soc Symp Proc* 1990, 171, 45.
12. Sinha, R. S.; Okamoto, M. *Prog Polym Sci* 2003, 28, 1539.
13. Ma, C. C. M.; Kuo, C. T.; Kuan, H. C.; Chiang, C. L. *J Appl Polym Sci* 2003, 88, 1686.
14. Sikdar, D.; Katti, D.; Katti, K.; Mohanty, B. *J Appl Polym Sci* 2007, 105, 790.
15. Katti, K. S. *Colloids Surf B Biointerfaces* 2004, 39, 133.
16. Vaia, R. A.; Pinnavaia, T. J.; Beall, G. W., Eds. *Polymer-Clay nanocomposites*; Wiley: New York, 2002; p 229.
17. Zeng, Q. H.; Yu, A. B.; Lu, G.; Standish, R. K. *Chem Mater* 2003, 15, 4732.
18. Chen, G.; Shen, D.; Feng, M.; Yang, M. *Macromol Rapid Commun* 2004, 25, 1121.
19. Gaudel-Siri, A.; Brocorens, P.; Siri, D.; Gardebien, F.; Bredas, J. L.; Lazzaroni, R. *Langmuir* 2003, 19, 8287.
20. Vaia, R. A.; Giannelis, E. P. *Macromolecules* 1997, 30, 8000.
21. Ginzburg, V. V.; Singh, C.; Balazs, A. C. *Macromolecules* 2000, 33, 1089.
22. Balazs, A. C. *Curr Opin Solid State Mater Sci* 2003, 7, 27.
23. Sikdar, D.; Katti, D. R.; Katti, K. S. *Langmuir* 2006, 22, 7738.
24. Sikdar, D.; Katti, D. R.; Katti, K. S.; Bhowmick, R. *Polymer* 2006, 47, 5196.
25. Brooks, B. R.; Brucoleri, R. E.; Olafson, B. D.; States, D. J.; Swaminathan, S.; Karplus, M. *J Comput Chem* 1983, 4, 187.
26. Skipper, N. T.; Sposito, G.; Chang, F. R. *Clays Clay Miner* 1995, 43, 285.
27. Skipper, N. T.; Sposito, G.; Chang, F. R. *Clays Clay Miner* 1995, 43, 294.
28. Teppen, B. J.; Rasmussen, K.; Bertsch, P. M.; Miller, D. M.; Schafer, L. *J Phys Chem B* 1997, 101, 1579.
29. Katti, D.; Schmidt, S.; Ghosh, P.; Katti, K. *Clays Clay Miner* 2005, 53, 171.
30. Humphrey, W.; Dalke, A.; Schulten, K. *J Mol Graph* 1996, 14, 33. Available at <http://www.ks.uiuc.edu/Research/vmd/>.
31. Katti, K.; Sikdar, D.; Katti, D.; Ghosh, P.; Verma, D. *Polymer* 2006, 47, 403.
32. Kalè, L.; Skeel, R.; Bhandarkar, M.; Brunner, R.; Gursoy, A.; Krawetz, N.; Phillips, J.; Shinozaki, A.; Varadarajan, K.; Schulten, K. *J Comput Phys* 1999, 151, 283. Available at <http://www.ks.uiuc.edu/research/namd/>.
33. Karasawa, N.; Goddard, W. A. *J Phys Chem* 1989, 93, 7320.
34. Martyna, G. J.; Tobias, D. J.; Klein, M. L. *J Chem Phys* 1994, 101, 4177.
35. Feller, S. E.; Zhang, Y.; Pastor, R. W.; Brooks, B. R. *J Chem Phys* 1995, 103, 4613.
36. Sikdar, D.; Katti, K. S.; Katti, D. R. *J. Nanosci Nanotechnol*, to appear.
37. Qin, H.; Zhang, S.; Zhao, C.; Yang, M. *J Polym Sci Part B: Polym Phys* 2005, 43, 3713.
38. Mitsunaga, M.; Ito, Y.; Ray, S. S.; Okamoto, M.; Hironaka, K. *Macromol Mater Eng* 2003, 288, 543.